Reducing the domain in the mechanical analysis of periodic structures, with application to woven composites

N.V. de Carvalho, S.T. Pinho, P. Robinson

Reducing the domain in the mechanical analysis of periodic structures, with application to woven composites

N.V. De Carvalho, S.T. Pinho, P. Robinson

PII: S0266-3538(11)00091-1
DOI: 10.1016/j.compscitech.2011.03.001
Reference: CSTE 4940

To appear in: *Composites Science and Technology*

Received Date: 15 December 2010
Revised Date: 27 February 2011
Accepted Date: 3 March 2011

Please cite this article as: De Carvalho, N.V., Pinho, S.T., Robinson, P., Reducing the domain in the mechanical analysis of periodic structures, with application to woven composites, *Composites Science and Technology* (2011), doi: 10.1016/j.compscitech.2011.03.001

Reducing the domain in the mechanical analysis of periodic structures, with application to woven composites.

N. V. De Carvalho[1], S. T. Pinho[1], P. Robinson[1]

[1] *Dept. of Aeronautics, Imperial College London, South Kensington, London, SW7 2AZ, UK*

Abstract

A theoretical framework is developped leading to a sound derivation of Periodic Boundary Conditions (PBCs) for the analysis of domains smaller then the Unit Cells (UCs), named reduced Unit Cells (rUCs), by exploiting non-orthogonal translations and symmetries. A particular type of UCs, Offset-reduced Unit Cells (OrUCs) are highlighted. These enable the reduction of the analysis domain of the traditionally defined UCs without any loading restriction. The relevance of the framework and its application is illustrated through practical examples: 2D woven laminates and 3D woven composites.

The framework proposed is used to develop an algorithm that automatically: (i) selects the smallest rUC for a given loading, (ii) determines and (iii) applies the appropriate periodic boundary conditions to the Finite Element Model (FEM). Coupled with a modelling/meshing tool, it provides a strategy for the efficient automatic numerical modelling and analysis of periodic structures. The algorithm is applied and validated for 2D woven orthogonal weaves. The results suggest the relevance of the proposed algorithm towards the efficient multiscale modelling of this class of materials.

Key words: A. Textile composites, C. Multiscale modelling, C. Finite element analysis (FEA), Unit cell

1. Introduction

Numerical analysis of periodic materials and structures has proven to be an extremely powerful tool. It has been successfully used to determine homogenised properties, study the detailed stress-strain fields at nano- and microscopic scales to obtain structural damage initiation conditions and sites, as well as to simulate damage development and associated deterioration of the homogenised mechanical

properties [1]. Several works can be found discussing the application of periodic boundary conditions to representative regions, e.g. [2–5]. For periodic structures, the Unit Cell (UC) is used as the representative region, and the analysis is performed by applying periodic displacement boundary conditions. The topological complexity of many UCs found in practice, such as in typical woven composites, often leads to unpractical modelling and analysis times. For this reason, internal symmetries of the UCs must whenever possible be exploited to reduce the analysis domain further (provided the appropriate boundary conditions are applied), thus reducing both modelling and analysis time.

A comprehensive study on the determination of reduced Unit Cells (rUCs) for UD and particle reinforced composites was performed by Li [6, 7] and Li and Wongsto [8]. Different rUCs, loading cases and correspondent boundary conditions were determined and presented in detail. Applied to textile composites, Tang and Whitcomb [9] proposed a general framework for determining rUCs.

In the first part of the present work, the derivation of the framework proposed in [9] is revisited and some of its building blocks redefined, resulting in a different, formally defined and more concise formulation. The framework proposed by Tang and Whitcomb [9] requires the distinction of two different cases of equivalence between subcells: (i) equivalence is obtained by a symmetry operation or a translation, and (ii) equivalence is obtained by the combination of a symmetry operation and a translation. In the second case an additional vector of constants $\mathbf{r}$ (see Tang and Whitcomb [9]) needs to be considered when applying the boundary conditions. The non-zero components of this vector are tabulated for different cases and are determined by the FEM as part of the solution. The formulation derived in the present work is more generic, in that no cases need to be treated separately, and mathematically complete in that no vector $\mathbf{r}$ needs to be determined from tabulated data. All terms in the equation that assigns the periodic boundary conditions for a rUC are fully defined, simplifying the formulation and consequently their use.

In this paper, the application of rUCs and their potential is illustrated through practical examples: 2D woven laminates, 3D woven composites. Particular attention is given to Offset-reduced Unit Cells. The importance of these types of unit cells was highlighted by Li for the analysis of UD composites [7]

and cracked laminates [10]. How they fit in the theoretical framework proposed and practical applications, namely in the domain reduction of 2D laminates and 3D woven composites, are highlighted.

The derivation of the boundary conditions for a given rUC and their implementation in FE can be a time-consuming process. In the final section of this paper, using the formulation developed, an algorithm is implemented which can: (i) identify the smallest rUC as a function of the prescribed loading, (ii) derive the boundary conditions for the rUC selected, (iii) implement the boundary conditions derived, preparing an input file to be analysed by the FE solver used. The algorithm is coupled with a voxel modelling/meshing procedure and applied to 2D woven orthogonal weaves, allowing the automatic numerical modelling and analysis of rUCs for this class of materials.

2. Equivalence framework

In this section, the equivalence framework is formally defined. It is based on four concepts: physical equivalence, load equivalence, periodicity and load admissibility. In the following sections each of these concepts is detailed.

2.1. Physical equivalence

Consider a domain $\mathbf{D}$ in space and within it a sub-domain E. The latter has a defined boundary, Local Coordinate System (LCS) $O_E xyz$, and a certain spatial distribution of n physical properties $\mathbf{P}^i$ with $i \in \{1, ..., n\}$. Each of these physical properties $\mathbf{P}^i$ are expressed as a tensor written in the LCS of E, i.e. $\mathbf{P}^i_E$.

Definition 1. *Two distinct sub-domains E and $\hat{E}$ are Physically Equivalent, denoted:*

$$E \widehat{=} \hat{E} \tag{1}$$

if for every point A in E there is a point $\hat{A}$ in $\hat{E}$ such that, for each physical property i,

$$\mathbf{x}^A_E = \mathbf{x}^{\hat{A}}_{\hat{E}} \wedge \mathbf{P}^i_E(A) = \mathbf{P}^i_{\hat{E}}\left(\hat{A}\right) \tag{2}$$

and vice-versa.

In Eq. 2, $\mathbf{x}^A_E$ and $\mathbf{x}^{\hat{A}}_{\hat{E}}$ are the coordinate vectors of A and $\hat{A}$ given in the LCS $O_E xyz$ and $O_{\hat{E}} xyz$ associated with E and $\hat{E}$, respectively. The points A and $\hat{A}$ for which Eq. 1 is verified are designated as physically equivalent points.

2.2. Periodicity and Unit Cell

Across the literature, different definitions can be found for periodic structure and UC. In the present work, periodic structure and UC are defined based on the concept of physical equivalence.

Definition 2. *A domain D is periodic if it can be reconstructed by tessellation of, non-overlapping, physically equivalent sub-domains E_i with parallel LCS (same versors), i.e. if for all $i \neq j$:*

$$E_i \widehat{=} E_j \wedge O_{E_i}xyz \parallel O_{E_j}xyz \tag{3}$$

The smallest sub-domain verifying the periodicity definition is designated as an Unit Cell.

2.3. Loading equivalence

The concept of load equivalence (see Tang and Whitcomb [9]) provides a relation between physically-equivalent sub-domains, once the structure they are part of is loaded. Let us consider a periodic structure as defined in the previous section.

Definition 3. *Load equivalence between two physically equivalent points A and $\hat{A}$ is verified if the strains and stresses at these points, given in the LCS of the sub-domains, can be related by:*

$$\varepsilon_E(A) = \gamma \varepsilon_{\hat{E}}\left(\hat{A}\right) \tag{4}$$

$$\sigma_E(A) = \gamma \sigma_{\hat{E}}\left(\hat{A}\right), \tag{5}$$

where the load reversal factor, $\gamma = \pm 1$, is used to enforce the equivalence between fields of physically equivalent sub-domains.

For Eqs. 4 and 5 to hold, the length scale of the loading variation must be larger than the length scale of the sub-domains, such that an approximately periodic variation of the strains and stress fields is assured. If a structure is entirely composed by load equivalent sub-domains, its response can be obtained by analysing one of these domains alone, instead of analysing the entire structure. However, the appropriate boundary conditions have to be applied. These guarantee that the sub-domain, although isolated, has the same response it would have if it was embedded in the structure.

2.4. Sub-domain admissibility

Not all physically equivalent sub-domains can be used to analyse the response of a periodic structure under all loading conditions. The use of sub-domains smaller than the UC to analyse the response of a periodic structure is restricted by the relations between the LCS of these sub-domains. The

sufficient and necessary condition for admissibility of a sub-domain to be used in the analysis of a periodic structure is derived below.

Average and fluctuation fields

For convenience, the strain field of a sub-domain at a point A is decomposed as the sum of a volume average and a fluctuation term:

$$\varepsilon\left(A\right) = \langle\varepsilon\rangle + \varepsilon^{*}\left(A\right), \tag{6}$$

where $\langle\bullet\rangle = \frac{1}{V}\int_{V} \bullet dV$ is the volume average operator over the volume V, and ε^{*} is the fluctuation term, see Suquet [11]. It is possible to find the displacements at a given point by integration of Eq. 6. Assuming small displacements and no rigid body rotations, the displacement relative to the origin of a LCS, attached to the subdomain, comes as:

$$\mathbf{u}\left(A\right) = \langle\varepsilon\rangle \cdot \mathbf{x}^{A} + \mathbf{u}^{*}\left(A\right). \tag{7}$$

Relations between fields of two equivalent points in a global coordinate system

Knowing that the coordinate vectors of two equivalent points A and $\hat{A}$ given in their LCSs are identical, Eq. 2, they can be related in the LCS of the sub-domain E by:

$$\mathbf{x}_{E}^{A} = \mathbf{T}\left(\mathbf{x}_{E}^{\hat{A}} - \mathbf{x}_{E}^{O_{\hat{E}}}\right) \tag{8}$$

where $\mathbf{T}$ is the transformation matrix between the LCSs of $\hat{E}$ and E, and $\mathbf{x}_{E}^{O_{\hat{E}}}$ is the position vector of the origin of the LCS of the sub-domain $\hat{E}$ given in the LCS of the sub-domain E, Fig. 1. Similarly, using Eq. 4, the strains at two equivalent points can be related in the LCS of E by:

$$\varepsilon_{E}\left(A\right) = \gamma\mathbf{T}\varepsilon_{E}\left(\hat{A}\right)\mathbf{T}^{t}. \tag{9}$$

The relation between the volume average of the strain of the equivalent sub-domains E and $\hat{E}$, in the LCS of the first, can be obtained directly by integrating Eq. 9:

$$\langle\varepsilon\rangle_{E}^{E} = \gamma\mathbf{T}\langle\varepsilon\rangle_{E}^{\hat{E}}\mathbf{T}^{t}, \tag{10}$$

where the lower index of $\langle\bullet\rangle$ refers to the coordinate system, and the upper index to the domain over

which the volume average was taken. Decomposing the strain field in Eq. 9 into its average and fluctuation parts and using Eq. 10, the relation between the strain fluctuations field of two equivalent points is obtained:

$$\varepsilon_E^*(A) = \gamma \mathbf{T} \varepsilon_{\hat{E}}^* \left(\hat{A}\right) \mathbf{T}^t. \tag{11}$$

A similar relation can be found for the displacement fluctuation fields:

$$\mathbf{u}_E^*(A) = \gamma \mathbf{T} \mathbf{u}_{\hat{E}}^* \left(\hat{A}\right) \tag{12}$$

details on the derivation of Eq. 12 can be found in [12].

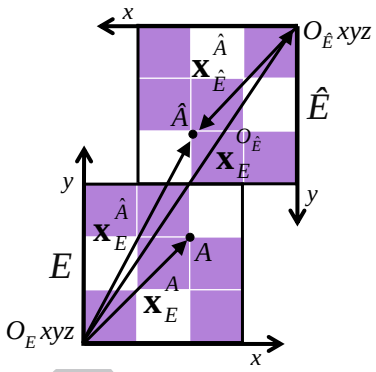

Figure 1: Geometrical relation between equivalent points.

Evaluation of the sub-domain admissibility

For a sub-domain to be admissible, the volume average (homogenised) strain calculated for this sub-domain on a given reference system must equal that volume average on any other sub-domain (on the same reference system), as the volume average is a homogenised entity, hence independent of the sub-domain where it was calculated. From load equivalence, the strains at physically-equivalent points are related (Eq. 5). Eq. 11 is obtained by simply integrating this relation over the sub-domain, but does not enforce directly that the volume average strain is a macroscopic entity independent of the particular sub-domain. For the sub-domain to be admissible, the following condition must be verified:

$$\langle \varepsilon \rangle_E^E = \langle \varepsilon \rangle_E^{\hat{E}} \tag{13}$$

as, for a sub-domain to be admissible, the homogenised strain on a given reference system (in this case E) must be the same for any sub-domain (in this case E and $\hat{E}$). Therefore, Eq. 10 with Eq. 13 lead to the condition of sub-domain admissibility, as defined below.

Definition 4. *A given sub-domain E is admissible for the analysis of a periodic structure under a given loading $\langle\varepsilon\rangle_E$, if $\mathbf{T}_i$ and γ_i correspondent to any other sub-domain $\hat{E}_i$ are such that, for all $\hat{E}_i$:*

$$\langle\varepsilon\rangle_E^E = \gamma_i \mathbf{T}_i \langle\varepsilon\rangle_E^{\hat{E}_i} \mathbf{T}_i^t \tag{14}$$

Equation 14 can be used to, for a given loading, determine the load reversal factors γ_i associated with each of the sub-domains. The admissibility of a subdomain for structural analysis leads to the definition of a rUC.

Definition 5. *A reduced Unit Cell is a domain, smaller than the Unit Cell, that can be used to determine the response of a periodic structure to a given loading. The condition to be verified by a reduced Unit Cell in structural analysis is defined by Eq. 14.*

3. Derivation of Periodic Boundary conditions

To ensure the response of a periodic structure under a given loading can be determined from the response of a rUC, the appropriate boundary conditions that must applied to the latter need to be determined. In this section, the equivalence framework, presented previously, is used to derive the periodic boundary conditions for the analysis of rUCs.

Consider two adjacent sub-domains E and $\hat{E}$ that are physically and load equivalent. If a point $\hat{A}$ belonging to $\hat{E}$ is chosen to be at the boundary of the sub-domain E, then its equivalent point A is also be at the boundary of E. Since both points A and $\hat{A}$ belong to E, the displacement at each point can be obtained using Eq. 7:

$$\mathbf{u}(A) = \langle\varepsilon\rangle \mathbf{x}^A + \mathbf{u}^*(A) \tag{15}$$

$$\mathbf{u}\left(\hat{A}\right) = \langle\varepsilon\rangle \mathbf{x}^{\hat{A}} + \mathbf{u}^*\left(\hat{A}\right) \tag{16}$$

All quantities in Eqs. 15 and 16 are written in the LCS of E, and the volume average is taken over the sub-domain E (the subscript will be omitted hereafter for convenience). Since both points are

equivalent, their positions are related by Eq. 8 leading to:

$$\mathbf{u}\left(A\right) = \left\langle \varepsilon \right\rangle \mathbf{T}\left(\mathbf{x}^{\hat{A}} - \mathbf{x}^{O_{\hat{E}}}\right) + \mathbf{u}^{*}\left(A\right) \tag{17}$$

Knowing that the displacement fluctuations at two equivalent points are related by Eq. 12, if Eq. 16 is multiplied by $\gamma\mathbf{T}$ and then subtracted to Eq. 15, the displacement fluctuations cancel, leading to:

$$\mathbf{u}\left(A\right) - \gamma\mathbf{T}\mathbf{u}\left(\hat{A}\right) = \left(\left\langle \varepsilon \right\rangle \mathbf{T} - \gamma\mathbf{T}\left\langle \varepsilon \right\rangle\right)\mathbf{x}^{\hat{A}} - \left\langle \varepsilon \right\rangle \mathbf{T}\mathbf{x}^{O_{\hat{E}}} \tag{18}$$

Provided the sub-domain $\hat{E}$ is admissible, see Definition 4, the term $\left(\left\langle \varepsilon \right\rangle \mathbf{T} - \gamma\mathbf{T}\left\langle \varepsilon \right\rangle\right)$ is zero. Using this result, Eq. 18 can be simplified to Eq. 19, which is the main outcome of this analysis and can be used directly to apply periodic boundary conditions to a sub-domain:

$$\mathbf{u}\left(A\right) - \gamma\mathbf{T}\mathbf{u}\left(\hat{A}\right) \quad = \quad - \left\langle \varepsilon \right\rangle \mathbf{T}\mathbf{x}^{O_{\hat{E}}} \tag{19}$$

Once a displacement constraint equation is associated to all points at the boundary of the sub-domain E, loading can be applied by prescribing a volume average strain $\left\langle \varepsilon \right\rangle$.

It is relevant to notice that the displacement constraint equation traditionally used to impose periodic boundary conditions on a UC, see Suquet [11] for example, is a particular case of Eq. 19 where the matrix $\mathbf{T}$ is equal to the identity matrix $\mathbf{I}$, since the LCSs of the UCs are parallel by definition and consequently, from the sub-domain admissibility evaluation, the load reversal factor is equal to one.

It is important to highlight the differences between the result obtained above and the one obtained in Tang and Whitcomb [9]; as referred before, Eq. 19 is completely generic and self sufficient: no distinction needs to be made, in the current formulation, between the type of operation needed to achieve equivalence between subdomains. Moreover, all terms in Eq. 19 are fully defined, and can therefore be readily used to prescribe periodic boundary conditions to a given subdomain. This is the first time a single equation is proposed for the definition of periodic boundary conditions exploiting symmetries for any periodic structure.

4. Applications

In the present section two applications of the formulation presented previously are illustrated. The first concerns a particular type of UCs, here named Offset-reduced Unit Cells, and their relevance for modelling woven laminates. The second emphasizes the relevance of OrUCs and rUCs for the domain reduction of 3D Woven composites.

4.1. 2D Woven Composites Laminates - Offset reduced Unit Cells

According to the periodicity definition given in 2.2, a UC is the smallest sub-domain that allows a periodic structure to be reconstructed by tessellation of sub-domains that are physically equivalent to the UC and have parallel LCS. Nevertheless, in most applications the UC is defined such that the LCS are not only parallel but orthogonally translated. However, smaller UCs can in general be defined if non-orthogonal translations are considered, Fig. 2a. Although, according to the definition, the representative sub-domains obtained through non-orthogonal translation are in fact UCs, in the present paper they are referred to as Offset-reduced Unit Cells, since they lead to a reduction in the domain of the traditionally defined UCs, Fig. 2a.

An important feature of OrUCs is that all loading combinations are admissible. This key feature has been identified by Li [7] and used in the derivation of PBCs for rUCs of UD composites, and cracked laminates [10]. It is relevant to highlight that using the present formulation this feature comes as a natural result: since the LCS of all sub-domains are parallel, they relate to each other by the identity matrix, i.e. $\mathbf{T} = \mathbf{I}$, as a consequence Eq. 14 is always verified and therefore all loading cases are admissible. In addtion to providing a domain reduction without load restriction, when applied to woven composites, OrUCs are particularly useful to model woven laminates. The relevance of modelling more than a single layer, and the effect of shifts between layers and consequent nesting has been reported in different works [13–15]. However, the modelling and analysis of a UC of the entire laminate is extremely time consuming. Provided all layers have the same orientation, OrUCs can be used to model laminates including the effect of shifts between layers and/or nesting of adjacent layers, leading to significant time savings.

In Fig. 2a, a 2×2 twill laminate is shown. If all laminae have the same orientation, it is possible to define a OrUC for the laminate, E of Fig. 2a. This OrUC has the laminate thickness and the same in-plane size as the OrUC of a laminae, Fig. 2b. It is independent of the shifts of the layers composing the laminate and of the nesting of adjacent layers. This can be seen observing that the sub-domains E and $\hat{E}_1$ are physically equivalent, Fig.2a. As mentioned above, $\mathbf{T} = \mathbf{I}$ and thus $\gamma_i = 1$, for all equivalent subdomains at the boundary of the OrUC. Therefore, the only variables needed to fully define Eq. 19, and prescribe the periodic boundary conditions to the OrUC, are the loading and the geometric relations between equivalent points at its boundary. The latter are obtained applying Eq. 8 to the equivalent domains at the boundary of the OrUC, and are provided in Table 1.

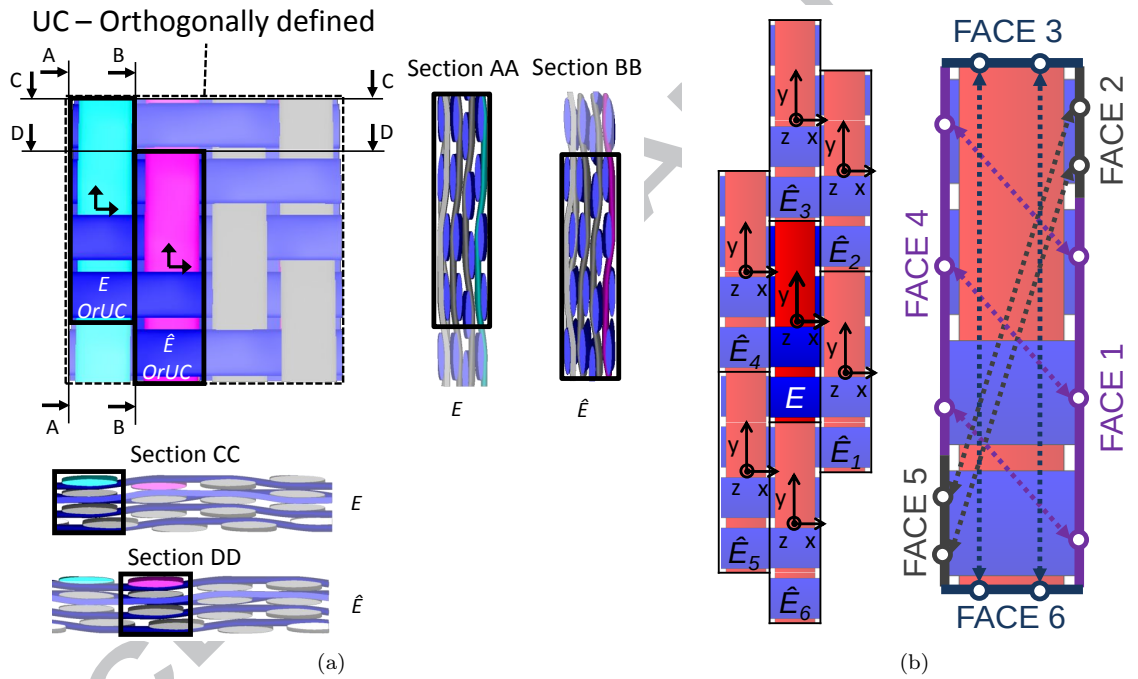

Figure 2: a) shows E and $\hat{E}$ are physically equivalent OrUCs for a 2×2 twill 0° warp-aligned random-shifted laminate b) shows how E can be used to reconstruct the weave using non-orthogonal translations and the geometrical relations between equivalent points at the boundary of E.

Table 1: Geometrical relations between equivalent points at the boundary for the 2×2 twill OrUC. l, w and t are respectively, the length width and and thickness of the OrUC.

	$\hat{E}_1$	$\hat{E}_2$	$\hat{E}_3$	$\hat{E}_4$	$\hat{E}_5$	$\hat{E}_6$
$\mathbf{x}^{O_{\hat{E}}}$	$\begin{bmatrix} w \\ -\frac{l}{4} \\ 0 \end{bmatrix}$	$\begin{bmatrix} w \\ \frac{3l}{4} \\ 0 \end{bmatrix}$	$\begin{bmatrix} 0 \\ l \\ 0 \end{bmatrix}$	$\begin{bmatrix} -w \\ \frac{l}{4} \\ 0 \end{bmatrix}$	$\begin{bmatrix} -w \\ -\frac{3l}{4} \\ 0 \end{bmatrix}$	$\begin{bmatrix} 0 \\ -l \\ 0 \end{bmatrix}$
$\mathbf{x}^{\hat{A}}$	$\begin{bmatrix} x=\frac{w}{2} \\ -\frac{l}{2} \le y \le \frac{l}{4} \\ -\frac{t}{2} \le z \le \frac{t}{2} \end{bmatrix}$	$\begin{bmatrix} x=\frac{w}{2} \\ \frac{l}{4} \le y \le \frac{l}{2} \\ -\frac{t}{2} \le z \le \frac{t}{2} \end{bmatrix}$	$\begin{bmatrix} -\frac{w}{2} \le x \le \frac{w}{2} \\ y=\frac{l}{2} \\ -\frac{t}{2} \le z \le \frac{t}{2} \end{bmatrix}$	$\begin{bmatrix} x=-\frac{w}{2} \\ -\frac{l}{4} \le y \le \frac{l}{2} \\ -\frac{t}{2} \le z \le \frac{t}{2} \end{bmatrix}$	$\begin{bmatrix} x=-\frac{w}{2} \\ -\frac{l}{2} \le y \le -\frac{l}{4} \\ -\frac{t}{2} \le z \le \frac{t}{2} \end{bmatrix}$	$\begin{bmatrix} -\frac{w}{2} \le x \le \frac{w}{2} \\ y=-\frac{l}{2} \\ -\frac{t}{2} \le z \le \frac{t}{2} \end{bmatrix}$
$\mathbf{x}^{A}$	$\begin{bmatrix} x_1^{\hat{A}} - w \\ x_2^{\hat{A}} + \frac{l}{4} \\ x_3^{\hat{A}} \end{bmatrix}$	$\begin{bmatrix} x_1^{\hat{A}} - w \\ x_2^{\hat{A}} - \frac{3l}{4} \\ x_3^{\hat{A}} \end{bmatrix}$	$\begin{bmatrix} x_1^{\hat{A}} \\ x_2^{\hat{A}} - l \\ x_3^{\hat{A}} \end{bmatrix}$	$\begin{bmatrix} x_1^{\hat{A}} + w \\ x_2^{\hat{A}} - \frac{l}{4} \\ x_3^{\hat{A}} \end{bmatrix}$	$\begin{bmatrix} x_1^{\hat{A}} + w \\ x_2^{\hat{A}} + \frac{3l}{4} \\ x_3^{\hat{A}} \end{bmatrix}$	$\begin{bmatrix} x_1^{\hat{A}} \\ x_2^{\hat{A}} + l \\ x_3^{\hat{A}} \end{bmatrix}$

4.2. 3D Woven Composites

The UCs of 3D woven composites can be significantly larger than their 2D counterparts, mostly due to the more intricate reinforcement architecture and 3D nature. Therefore, the domain reduction enabled by the use of rUCs can be very significant. Figure 3a shows an UC, an OrUC and a rUC of a given 3D woven architecture, highlighting the domain reduction achieved: OrUC and rUC reduce the analysis domain to $1/7$ and $1/28$ of the UC, respectively.

To define the periodic boundary conditions for the analysis of the rUC of Fig. 3, Eq. 19, the geometric relations between equivalent points at the rUC boundary need to be found. These are obtained, similarly to the OrUC case, by applying Eq. 8 to the equivalent domains at the boundary of the rUC and are given in Table 2 and illustrated in Fig. 3b. Since in general, $\mathbf{T} \neq \mathbf{I}$, the load admissibility needs to be evaluated and γ, for each adjacent subdomain, determined. This is performed evaluating Eq. 14, and summarized in Table 3. Given a certain loading and using the data from Tables 2 and 3, Eq. 19 can be fully defined and periodic boundary conditions prescribed to the rUC.

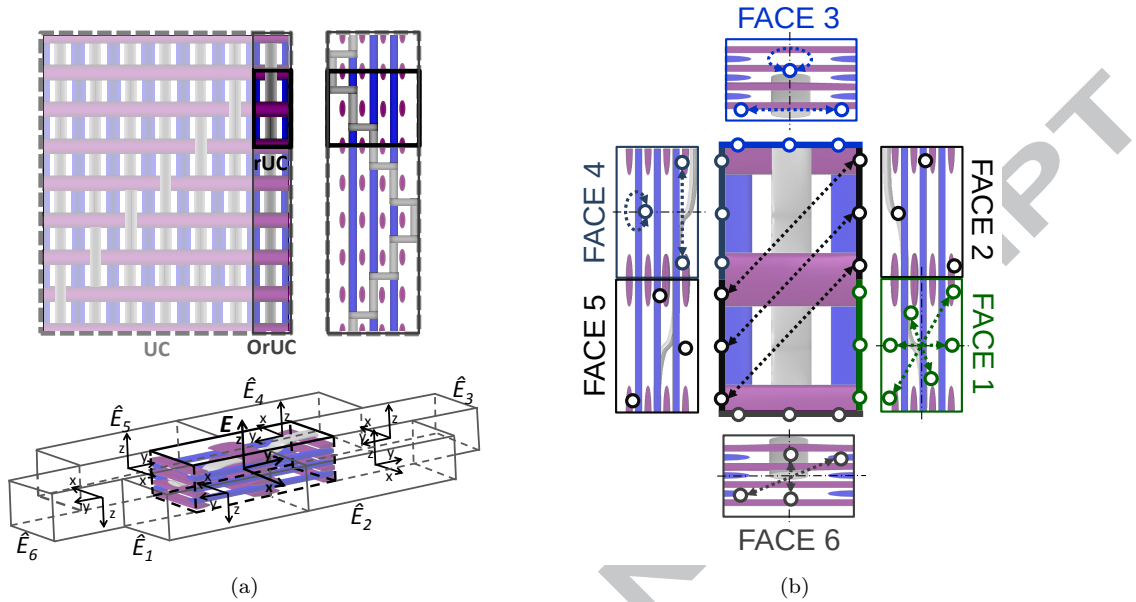

(a) (b)

Figure 3: a) UC, OrUC and rUC of a 3D woven reinforcement architecture; representation of the reduced Unit Cell (rUC) and adjacent sub-domains, b) geometrical relations between equivalent points at the boundary of the rUC.

Table 2: Geometrical relations between equivalent points at the boundary for the 3D woven rUC. l, w and t are respectively, the length width and and thickness of the rUC.

	$\hat{E}_1$	$\hat{E}_2$	$\hat{E}_3$	$\hat{E}_4$	$\hat{E}_5$	$\hat{E}_6$
$\mathbf{T}$	$\begin{bmatrix} -1 & 0 & 0 \\ 0 & -1 & 0 \\ 0 & 0 & -1 \end{bmatrix}$	$\begin{bmatrix} 1 & 0 & 0 \\ 0 & 1 & 0 \\ 0 & 0 & 1 \end{bmatrix}$	$\begin{bmatrix} -1 & 0 & 0 \\ 0 & -1 & 0 \\ 0 & 0 & 1 \end{bmatrix}$	$\begin{bmatrix} -1 & 0 & 0 \\ 0 & -1 & 0 \\ 0 & 0 & 1 \end{bmatrix}$	$\begin{bmatrix} 1 & 0 & 0 \\ 0 & 1 & 0 \\ 0 & 0 & 1 \end{bmatrix}$	$\begin{bmatrix} -1 & 0 & 0 \\ 0 & -1 & 0 \\ 0 & 0 & -1 \end{bmatrix}$
$\mathbf{x}^{O_{\hat{E}}}$	$\begin{bmatrix} w \\ -\frac{l}{2} \\ 0 \end{bmatrix}$	$\begin{bmatrix} w \\ \frac{l}{2} \\ 0 \end{bmatrix}$	$\begin{bmatrix} 0 \\ l \\ 0 \end{bmatrix}$	$\begin{bmatrix} -w \\ \frac{l}{2} \\ 0 \end{bmatrix}$	$\begin{bmatrix} -w \\ -\frac{l}{2} \\ 0 \end{bmatrix}$	$\begin{bmatrix} 0 \\ -l \\ 0 \end{bmatrix}$
$\mathbf{x}^{\hat{A}}$	$\begin{bmatrix} x = \frac{w}{2} \\ -\frac{l}{2} \leq y \leq 0 \\ -\frac{t}{2} \leq z \leq \frac{t}{2} \end{bmatrix}$	$\begin{bmatrix} x = \frac{w}{2} \\ 0 \leq y \leq \frac{l}{2} \\ -\frac{t}{2} \leq z \leq \frac{t}{2} \end{bmatrix}$	$\begin{bmatrix} -\frac{w}{2} \leq x \leq \frac{w}{2} \\ y = \frac{l}{2} \\ -\frac{t}{2} \leq z \leq \frac{t}{2} \end{bmatrix}$	$\begin{bmatrix} x = -\frac{w}{2} \\ 0 \leq y \leq \frac{l}{2} \\ -\frac{t}{2} \leq z \leq \frac{t}{2} \end{bmatrix}$	$\begin{bmatrix} x = -\frac{w}{2} \\ -\frac{l}{2} \leq y \leq 0 \\ -\frac{t}{2} \leq z \leq \frac{t}{2} \end{bmatrix}$	$\begin{bmatrix} -\frac{w}{2} \leq x \leq \frac{w}{2} \\ y = -\frac{l}{2} \\ -\frac{t}{2} \leq z \leq \frac{t}{2} \end{bmatrix}$
$\mathbf{x}^{A}$	$\begin{bmatrix} w - x_1^{\hat{A}} \\ -\frac{l}{2} - x_2^{\hat{A}} \\ -x_3^{\hat{A}} \end{bmatrix}$	$\begin{bmatrix} x_1^{\hat{A}} - w \\ x_2^{\hat{A}} - \frac{l}{2} \\ x_3^{\hat{A}} \end{bmatrix}$	$\begin{bmatrix} -x_1^{\hat{A}} \\ -x_2^{\hat{A}} + l \\ x_3^{\hat{A}} \end{bmatrix}$	$\begin{bmatrix} -x_1^{\hat{A}} - w \\ -x_2^{\hat{A}} + \frac{l}{2} \\ x_3^{\hat{A}} \end{bmatrix}$	$\begin{bmatrix} x_1^{\hat{A}} + w \\ x_2^{\hat{A}} + \frac{l}{2} \\ x_3^{\hat{A}} \end{bmatrix}$	$\begin{bmatrix} -x_1^{\hat{A}} \\ -x_2^{\hat{A}} - l \\ -x_3^{\hat{A}} \end{bmatrix}$

Table 3: Admissible loading cases and respective value of the load reversal factor γ_i, correspondent to each adjacent sub-domain $\hat{E}_i$, for the 3D woven rUC.

	γ_i	Admissible loading
Case 1	$\begin{bmatrix} 1 & 1 & 1 & 1 & 1 & 1 \end{bmatrix}$	$\begin{bmatrix} \sigma_{11} & \sigma_{12} & 0 \\ \sigma_{21} & \sigma_{22} & 0 \\ 0 & 0 & \sigma_{33} \end{bmatrix}$
Case 2	$\begin{bmatrix} 1 & 1 & -1 & -1 & 1 & 1 \end{bmatrix}$	$\begin{bmatrix} 0 & 0 & \sigma_{13} \\ 0 & 0 & \sigma_{23} \\ \sigma_{31} & \sigma_{32} & 0 \end{bmatrix}$

5. Algorithm: Automatic detection of rUC and Finite Element Analysis applied to 2D Woven Composites

The finite element modelling and analysis of a rUC involves 5 steps: (i) selection of the smallest rUC for the loading applied, (ii) modelling and (iii) meshing of the geometry, (iv) derivation of the PBCs for the loading applied and rUC selected and (v) application of the PBCs as displacement constraints at the boundary of the rUC domain. In the present section, an algorithm is presented which is capable of: (i) automatically selecting the smallest rUC for the loading to be applied (ii) derive and (iii) apply the appropriate periodic boundary conditions for the rUC selected. The algorithm is implemented in Matlab®. In a first instance, given the loading to be applied, it provides the user with the information on the minimum domain necessary to model - dashed box "rUC" in Fig. 4. This saves modelling/meshing time and, at a later stage, analysis time. After the FE model is generated [16], the algorithm derives and applies the boundary conditions to the model, producing an input file ready to be analysed by the FE solver used, ABAQUS/Standard® - dashed box "PBC" in Fig. 4. The algorithm can be applied to any 2D orthogonal weave. Moreover, it important to highlight that its primitives are completely general and can therefore be extended to any periodic structure. In the following sections, the inputs and the two main blocks of the algorithm, "rUC" and "PBC" are examined in detail.

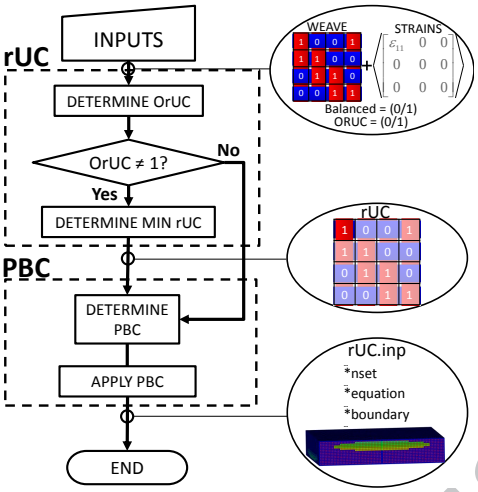

Figure 4: Flowchart of the algorithm

5.1. Inputs to the algorithm - "INPUTS"

The inputs needed to apply the algorithm are summarized in Table 4. The variable WEAVE contains the binary representation of the weave, Fig. 4. The nature of 2D orthogonal weaves, where the warp tow is either under (0) or over (1) the weft tow is particularly suitable for a binary representation. This enables the weave pattern recognition while requiring the minimum amount of information from the user. Besides the binary weave description, it is also necessary to define if the warp tows are identical to weft tows (properties, thickness, width, spacing, amongst others) as this affects the allowable symmetry operations. In the context of the present algorithm, this information is provided by the variable BALANCED. The user is also given the possibility of determining the boundary conditions for the OrUC of the unit cell being analyzed, by prescribing the variable ORUC equal to one. Finally the input variable STRAINS prescribes the volume average strains that are applied.

Table 4: Inputs for the algorithm

Variable	Type	Description
WEAVE	Matrix of integers	Binary description of the weave
BALANCED	Boolean	Defines if the weave is balanced (1) or unbalanced (0)
ORUC	Boolean	Defines if the rUC to be determined is a OrUC (1) or the minimum rUC (0) admissible
STRAINS	Matrix of doubles and characters	Volume averaged strains to be applied. If a component is to be found as a result of the analysis, a scalar c is prescribed in that component position.

5.2. Determination of the rUC - "rUC"

In the present section the scheme used to determine the rUC for a given input is detailed, Fig. 5. It is composed by two procedures: "DETERMINE OrUC" and "DETERMINE MIN rUC". Their overall description is made in Sections 5.2.1 and 5.2.2. Specific operations performed whithin these procedures are detailed in Section 5.2.3. Of these, the function "PHYS & LOAD EQ" is worth highlighting. This function evaluates if a given domain E is an (O)rUC, it is central to both procedures and therefore crucial to the algorithm, Fig. 5.

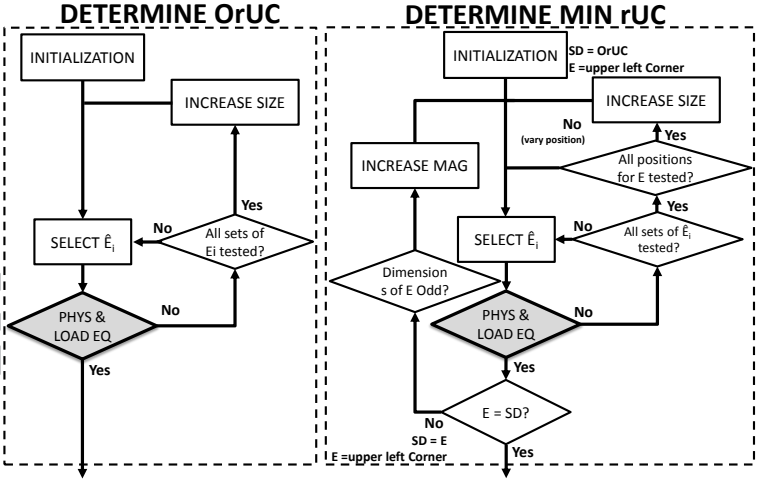

Figure 5: Detailed fluxogram of the procedures "DETERMINE OrUC" and "DETERMINE MIN rUC"

5.2.1. Determination of the OrUC - "DETERMINE OrUC"

In the "INITIALIZATION" procedure, the Selection Domain (SD), i.e. the domain within which the OrUC is searched for, is defined as the UC and the sub-domain E assumed to be a single digit located in the upper left corner of the SD. Next, the procedure "SELECT $\hat{E}_i$" selects a set of sub-domains at the boundary of E. The procedure "PHYS & LOAD EQ" checks if all the selected sub-domains are physically and load equivalent to E, (with $\mathbf{T} = \mathbf{I}$). If not, a different set of sub-domains is selected and the procedure repeated. If all possible sets of sub-domains at the boundary of the sub-domain E are tested without success, the given sub-domain is not a OrUC and the size of the sub-domain E is increased - "INCREASE SIZE". This process is repeated until a OrUC is found, i.e. for a given E all sub-domains $\hat{E}_i$ of the set being considered are physically and load equivalent to E. In the worst case, E will coincide with the SD, previously defined as the UC.

5.2.2. Determination of the minimum rUC - "DETERMINE MIN rUC"

Having found an OrUC, existent symmetries within the OrUC are exploited to further reduce the analysis domain. In the "INITIALIZATION" procedure, the OrUC is defined as the SD and E assumed to be a single digit located in the upper left corner of the SD. Next, the procedure "SELECT $\hat{E}_i$" selects a set of sub-domains at the boundary of E. The procedure "PHYS & LOAD EQ" checks if all the selected sub-domains are physically and load equivalent to E. If not, a new set $\hat{E}_i$ is selected and this process repeated. In case all possible sets of $\hat{E}_i$ are unsuccessfully evaluated the position of E within the selection domain is varied. Finally, if all possible locations and for each location all possible sets of $\hat{E}_i$ are unsuccessfully evaluated the sub-domain size is increased - "INCREASE SIZE" - and the process repeated for the new sub-domain E. If a rUC is found - all sub-domains $\hat{E}_i$ of the set being considered are physically and load equivalent to E - the selection domain (previously the OrUC) becomes E. Additionally, if the size in digits of any of sides of the newly found selection-domain is an odd number, the weave representation is magnified - "INCREASE MAG" and the new E is again assumed to be a single digit located in the upper left corner of the SD. The procedure terminates when the rUC found coincides with the SD.

5.2.3. Details on the operations performed to determine the OrUC and the minimum rUC

In this section the functions used by the procedures "DETERMINE OrUC" and "DETERMINE MIN rUC" are detailed.

Selection of a set of sub-domains $\hat{E}_i$ at the boundary of E - "SELECT $\hat{E}_i$"

Depending on the size and shape of a given sub-domain E, more than one set of sub-domains might be possible to select at its boundary, Fig. 6. The sets having the smaller number of sub-domains are evaluated first. This allows the minimization of the number of sub-domains that are necessary to evaluate. Additionally, it also minimizes the number of sub-domains needed to consider in the boundary conditions definition. In Fig. 6, case one has the minimum number of sub-domains at the boundary, however two sub-domains, $\hat{E}_1$ and $\hat{E}_3$ are not physically equivalent to the sub-domain, see Section 5.2.3. In cases two and four, all sub-domains at the boundary are physically equivalent to E. However, the transformations required by sub-domains $\hat{E}_1$ and $\hat{E}_4$ to be physically equivalent to E are different for the different cases. Depending on the loading and symmetry requirements one of the two cases (or both) might not be suitable.

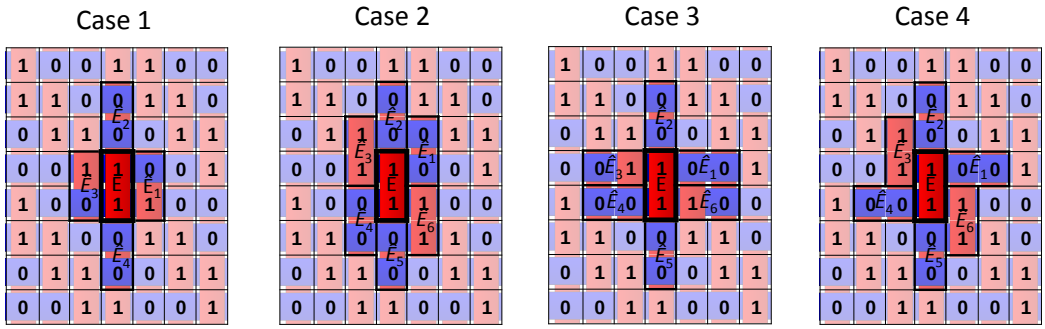

Figure 6: Different possibilities for defining the sub-domains at the boundary

Increase the size of the sub-domain E - "INCREASE SIZE"

The increase in size of the sub-domain E is performed progressively while minimizing the sub-domain area. It considers both square and rectangular sub-domains. The process is illustrated in Fig. 7a.

Increase the magnification of the selection domain - "INCREASE MAG"

The magnification of the binary representation is made by subdividing each digit of the selection domain in four digits with the same value, see Fig. 7b. Together with the sub-domain selection procedure, it enables any existent symmetries relative to the centre of the selection domain to be exploited. Moreover, it allows sub-domains smaller than one digit to be considered.

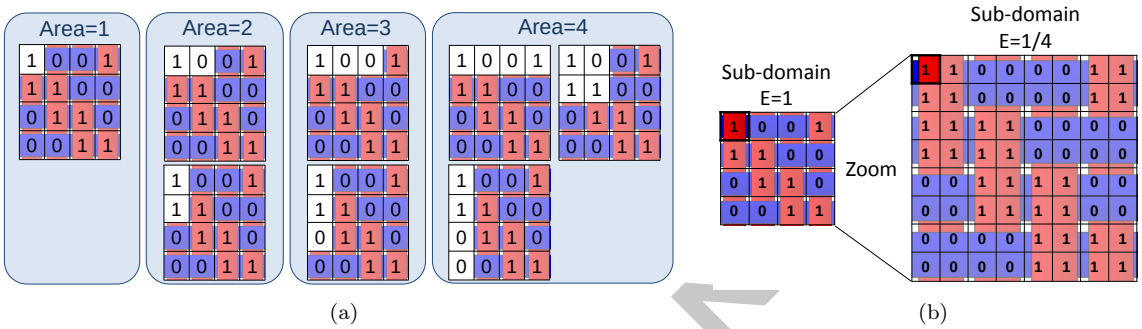

Figure 7: a) Progressive increase of the sub-domain area. For the same area more than one sub-domain can be selected. b) magnification of the weave representation

Evaluation of the physical and load equivalence between a domain E and a set of domains $\hat{E}_i$ at its boundary - "PHYS & LOAD EQ"

To determine if two regions of the weave are physically equivalent (identical geometry and material distribution) and the symmetry operations needed to achieve this equivalence it is necessary to: (i) compare their binary representation, (ii) evaluate if their positions within the weave geometry are equivalent. The later leads to the need of comparing domains larger than the sub-domains named Comparison Domains (CDs). This is illustrated in Fig. 8. The sub-domains $\hat{E}_3$ and $\hat{E}_4$ have the same binary representation of the domain E; if the position of the sub-domains within the weave was not considered it could be concluded that they were physically equivalent, without the need of any symmetry operation to obtain that equivalence. However, analyzing the weave geometry it is possible to see the positions of the sub-domains $\hat{E}_3$ and $\hat{E}_4$ within the weave geometry are not equivalent.

A Comparison Domain (CD) is defined such that: (i) it contains one complete UC; (ii) the sub-domain to be compared is at its centre. The UC fully defines the weave geometry; having one complete UC within the comparison domain ensures that the equivalence between the sub-domains positions

within the weave geometry can be assessed. Defining the CD in such way that the sub-domain is always at its centre facilitates the comparison between transformed sub-domains, since symmetry operations do not alter the sub-domain position within the comparison domain. Considering the upper left digit of the sub-domain (for sub-domains with more than one digit) to be in the position $i = 0$, $j = 0$, the limits of the CD for any sub-domain are given by:

$$\begin{cases} CD_{max_i} & = UC_{size_i} \\ CD_{min_i} & = -\left(UC_{size_i} - SD_{size_i}\right) \end{cases}, \text{ and } \begin{cases} CD_{max_j} & = UC_{size_j} \\ CD_{min_j} & = -\left(UC_{size_j} - SD_{size_j}\right) \end{cases}, \tag{20}$$

where UC_{size_k} and SD_{size_k} refer to the unit cell and sub-domain sizes, measured in number of digits, on the directions $k = i, j$. For the case illustrated in Fig. 8 the $UC_{size_i} = UC_{size_j} = 4$ and $SD_{size_i} = SD_{size_j} = 1$.

The use of the comparison domains to assess the geometrical equivalence is illustrated in Fig. 9 for the sub-domains E and $\hat{E}_3$. For the sub-domain E in Fig. 9 the CD is is given as in Fig. 8 and repeated in Fig. 9 for convenience. Using Eq. 20, the CD of the sub-domain $\hat{E}_3$ is defined similarly and illustrated in Fig. 9. Figure 9 shows that the CDs of the two sub-domains are different. The next step is to find a transformation that can make them identical. In this case, such a transformation exists and is defined by the matrix $\mathbf{T}$. As shown in Fig. 9, the transformed CD $\hat{E}_3'$ is identical to E and, therefore, physically equivalent. This procedure is repeated for all sub-domains at the boundary of the original sub-domain E. After assessing the physical equivalence, it is necessary to evaluate if the transformations obtained are admissible having into account the loading requirements. This evaluation is performed by ensuring Eq. 14 holds for all $\mathbf{T}_i$ and γ_i corresponding to the sub-domains $\hat{E}_i$, having into account the transformations obtained and the applied loading. This evaluation is exemplified using the sub-domains E and $\hat{E}_3$ of Fig. 9 and an applied loading:

$$\langle \varepsilon \rangle_E = \left\langle \begin{bmatrix} \varepsilon_{11} & 0 & 0 \\ 0 & 0 & 0 \\ 0 & 0 & c \end{bmatrix} \right\rangle, \tag{21}$$

given in the local coordinate system (LCS) of the sub-domain E. A non-zero value is prescribed to $\langle \varepsilon_{11} \rangle$, while $\langle \varepsilon_{33} \rangle = c$ is computed as an output of the FE simulation, allowing Poisson ratio expansion on the through-thickness direction. The LCS of the sub-domain $\hat{E}_3$ is related to LCS of E by $\mathbf{T}$ given in Fig. 9; substituting it in Eq. 14 one obtains:

$$\left\langle \begin{bmatrix} \varepsilon_{11} & 0 & 0 \\ 0 & 0 & 0 \\ 0 & 0 & c \end{bmatrix} \right\rangle = \gamma \left\langle \begin{bmatrix} \varepsilon_{11} & 0 & 0 \\ 0 & 0 & 0 \\ 0 & 0 & c \end{bmatrix} \right\rangle . \tag{22}$$

Taking $\gamma = 1$, Eq. 22 holds. Therefore, for the applied loading $\langle \varepsilon \rangle_E$ and for transformation $\mathbf{T}$ relating the LCSs of the two sub-domains, the loading equivalence between E and $\hat{E}_3$ is verified.

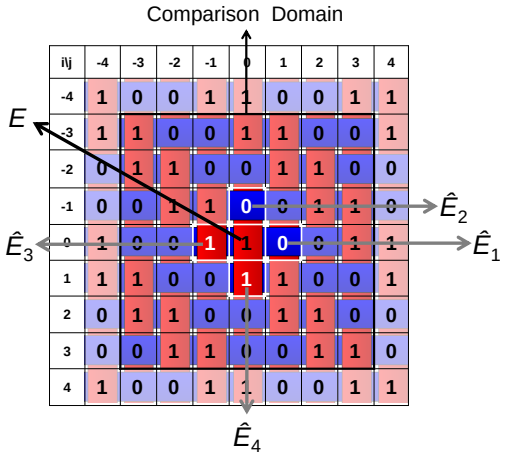

Figure 8: Comparison domain for the sub-domain at the position $i = j = 0$

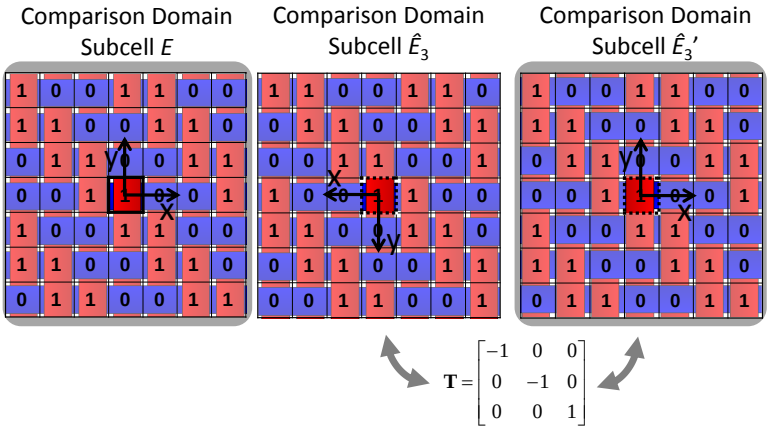

Figure 9: Comparison domains. Once transformed by $\mathbf{T}$ the comparison domain E_3' is identical to E, and therefore physically equivalent.

The transformation that leads to the sub-domain loading equivalence is searched within a set of

admissible symmetry operations. Due to the rectangular nature of the binary representation, only mirroring on different axis and straight angles rotations are allowed. Their combination leads to twelve independent transformations, eight when $\theta = 0\,\text{or}\,\pi$ and four when $\theta = \frac{\pi}{2}$ or $\frac{3\pi}{2}$:

$$\mathbf{T}_{\theta=0\ or\ \pi} = \begin{bmatrix} \pm1 & 0 & 0 \\ 0 & \pm1 & 0 \\ 0 & 0 & \pm1 \end{bmatrix}, \mathbf{T}_{\theta=\frac{\pi}{2}\ or\ \frac{3\pi}{2}} = \begin{bmatrix} 0 & \pm1 & 0 \\ \pm1 & 0 & 0 \\ 0 & 0 & 1 \end{bmatrix} \tag{23}$$

For $\theta = \frac{\pi}{2}$ or $\frac{3\pi}{2}$ rotations, mirroring on the z direction is not admissible due to the orthogonal nature of the weaves. If the warp yarns are not equivalent to the weft yarns (BALANCED = 0), $\theta = \frac{\pi}{2}$ or $\frac{3\pi}{2}$ rotations are not allowed. Additionally, by assigning ORUC = 1, the user can choose to make the analysis using an Offset-reduced Unit Cell. This implies that no symmetry operations can be performed and thus the matrix $\mathbf{T}$ is equal to the identity matrix.

5.3. Determination and implementation of the PBCs - "PBC"

In this section details are given on the steps needed to derive and apply PBCs to a FEM of a rUC, the procedures "DETERMINE PBC" and "APPLY PBC", respectively, Fig. 4.

5.3.1. Determination of the PBCs - "DETERMINE PBC"

As a result of the algorithm used to determine the (O)rUC, all variables needed to determine the PBCs, Eq. 19, are known or can be readily determined. The sign of γ and the matrix $\mathbf{T}$ are obtained directly from the equivalence evaluation. The vector $\mathbf{x}^{\hat{A}}$ refers to the points at the common boundary between the sub-domain being analyzed E and an adjacent sub-domain $\hat{E}$. The vector $\mathbf{x}^{A}$, is determined by Eq. 8 and comprises of the points equivalent to $\mathbf{x}^{\hat{A}}$ also located at the boundary of E. Finally, since the positions of all sub-domains are also known, the vector $\mathbf{x}^{O_{\hat{E}}}$ can be readily determined.

5.3.2. Implementation of the PBCs in a FEM - "APPLY PBC"

Periodic boundary conditions are imposed as displacement constraint equations, and written by the algorithm directly in the input file to be analysed by the FE solver. The algorithm, selects automatically the regions (nodes), at the boundary of the domain, that need to be coupled by the displacement constraints. This information is then written in the input file to be analysed by the FE solver. This selection is based on the values of $\mathbf{x}^{\hat{A}}$ and $\mathbf{x}^{A}$ obtained for the rUC being considered.

Depending on the rUC considered, the displacement-constraint equations will couple different regions: (i) different faces, (ii) regions belonging to the same face. In the first case, this implies the number of nodes on each face has to be the same. Moreover, if no symmetry operations are involved, the nodes in each face must be in identical positions. Often, the evaluation of the geometrical relation between equivalent points dictates a certain symmetry operation on the coupling between nodes of opposite faces. In this case the nodes do not necessarily need to be in identical positions, nevertheless their relative positions must respect the symmetry operation given. Figure 10a exemplifies the coupling of two opposite faces, with symmetry in the z direction (this can also be seen in the Fig. 11b faces 3 and 6). When the displacement-constraint equation is applied to nodes of the same face, it is only necessary to guarantee that the node distribution respects any symmetry operation given. In Fig. 10b this is exemplified for a case where symmetry is prescribed in the x direction (this can also be seen in Fig. 12b face 3). The ordered nature of voxel meshing used guarantees the requirements above mentioned. If other type of meshing is used, then the above requirements need to be considered carefully when meshing.

Parts of the boundary that belong to more than two sub-domains, (such as corners and edges) have two or more equations being applied. This leads to a redundant system of equations. To avoid this, these areas are considered separately and the linearly dependent equations are eliminated. The PBCs are finally implemented in ABAQUS/Standard® using the keyword *Equation [17]. When using this keyword each term can only be used once. In cases where symmetry exists, the nodes in the symmetry axis, are coupled with themselves and thus repeated in the equation, Fig. 10b. To circumvent this issue, these nodes are considered separately.

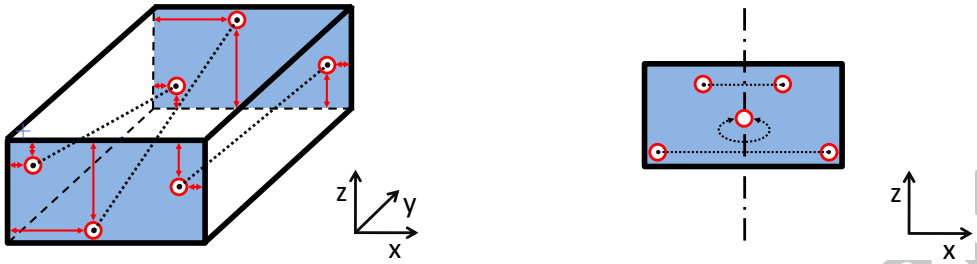

(a) (b)

Figure 10: a) Coupling of nodes belonging to different faces, with symmetry in z, and b) coupling of nodes belonging to the same face, with symmetry in x.

6. Results

This section illustrates the application of the algorithm to a practical case: the analysis of a 2×2 Twill woven ply.

6.1. Finite Element Analysis: 2×2 *Twill*

Figures 11 and 12 shows two rUCs obtained through the application of the algorithm: $\text{rUC}_{1/8}$ and $\text{rUC}_{1/16}$. These rUCs reduce the analysis domain to $1/8$ and $1/16$ of the Unit Cell, respectively. Tables 5 and 6 list the geometrical relations between equivalent points at the boundary of the rUCs illustrated Figs. 11 and 12. Table 7 shows the admissible loadings for the two rUCs. It is interesting to notice that both rUCs have the same load restrictions.

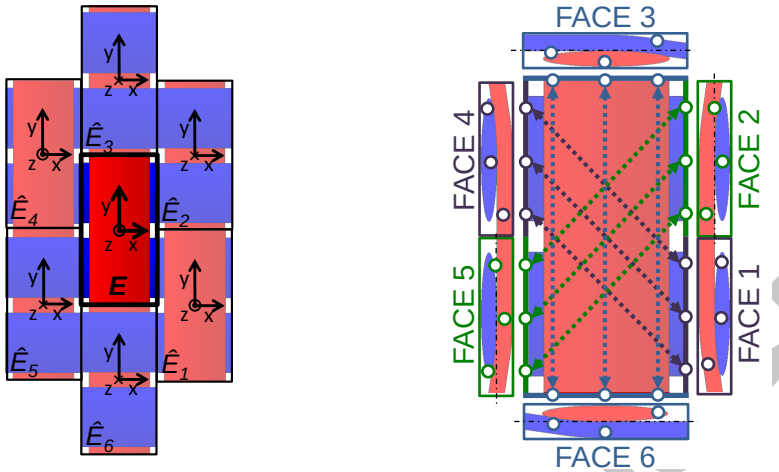

(a) (b)

Figure 11: rUC$_{1/8}$: a) Adjacent sub-domains, and b) geometrical relations between equivalent points at the boundary of the

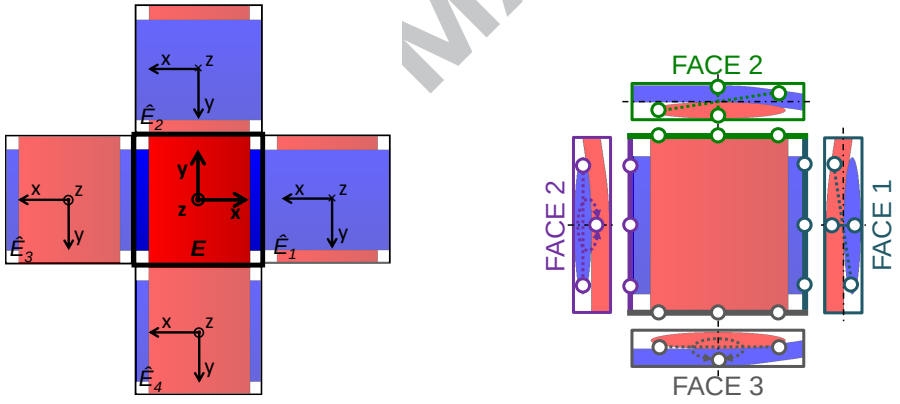

(a) (b)

Figure 12: rUC$_{1/16}$: a) Adjacent sub-domains, and b) geometrical relations between equivalent points at the boundary of the

Table 5: $\mathrm{rUC}_{1/8}$: geometrical relations between equivalent points at the boundaries; l, w and t are respectively, the length width and and thickness of the rUC.

	$\hat{E}_1$	$\hat{E}_2$	$\hat{E}_3$	$\hat{E}_4$	$\hat{E}_5$	$\hat{E}_6$
$\mathbf{T}$	$\begin{bmatrix} 1 & 0 & 0 \\ 0 & 1 & 0 \\ 0 & 0 & 1 \end{bmatrix}$	$\begin{bmatrix} 1 & 0 & 0 \\ 0 & 1 & 0 \\ 0 & 0 & -1 \end{bmatrix}$	$\begin{bmatrix} 1 & 0 & 0 \\ 0 & 1 & 0 \\ 0 & 0 & -1 \end{bmatrix}$	$\begin{bmatrix} 1 & 0 & 0 \\ 0 & 1 & 0 \\ 0 & 0 & 1 \end{bmatrix}$	$\begin{bmatrix} 1 & 0 & 0 \\ 0 & 1 & 0 \\ 0 & 0 & -1 \end{bmatrix}$	$\begin{bmatrix} 1 & 0 & 0 \\ 0 & 1 & 0 \\ 0 & 0 & -1 \end{bmatrix}$
$\mathbf{x}^{O_{\hat{E}}}$	$\begin{bmatrix} w \\ -\frac{l}{2} \\ 0 \end{bmatrix}$	$\begin{bmatrix} w \\ \frac{l}{2} \\ 0 \end{bmatrix}$	$\begin{bmatrix} 0 \\ l \\ 0 \end{bmatrix}$	$\begin{bmatrix} -w \\ \frac{l}{2} \\ 0 \end{bmatrix}$	$\begin{bmatrix} -w \\ -\frac{l}{2} \\ 0 \end{bmatrix}$	$\begin{bmatrix} 0 \\ -l \\ 0 \end{bmatrix}$
$\mathbf{x}^{\hat{A}}$	$\begin{bmatrix} \frac{w}{2} \\ -\frac{l}{2} \le y \le 0 \\ -\frac{t}{2} \le z \le \frac{t}{2} \end{bmatrix}$	$\begin{bmatrix} \frac{w}{2} \\ 0 \le y \le \frac{l}{2} \\ -\frac{t}{2} \le z \le \frac{t}{2} \end{bmatrix}$	$\begin{bmatrix} -\frac{w}{2} \le x \le \frac{w}{2} \\ y = \frac{l}{2} \\ -\frac{t}{2} \le z \le \frac{t}{2} \end{bmatrix}$	$\begin{bmatrix} -\frac{w}{2} \\ 0 \le y \le \frac{l}{2} \\ -\frac{t}{2} \le z \le \frac{t}{2} \end{bmatrix}$	$\begin{bmatrix} -\frac{w}{2} \\ -\frac{l}{2} \le y \le 0 \\ -\frac{t}{2} \le z \le \frac{t}{2} \end{bmatrix}$	$\begin{bmatrix} -\frac{w}{2} \le x \le \frac{w}{2} \\ y = -\frac{l}{2} \\ -\frac{t}{2} \le z \le \frac{t}{2} \end{bmatrix}$
$\mathbf{x}^{A}$	$\begin{bmatrix} x_1^{\hat{A}} - w \\ x_2^{\hat{A}} + \frac{l}{2} \\ x_3^{\hat{A}} \end{bmatrix}$	$\begin{bmatrix} x_1^{\hat{A}} - w \\ x_2^{\hat{A}} - \frac{l}{2} \\ -x_3^{\hat{A}} \end{bmatrix}$	$\begin{bmatrix} x_1^{\hat{A}} \\ x_2^{\hat{A}} - l \\ -x_3^{\hat{A}} \end{bmatrix}$	$\begin{bmatrix} x_1^{\hat{A}} + w \\ x_2^{\hat{A}} - \frac{l}{2} \\ x_3^{\hat{A}} \end{bmatrix}$	$\begin{bmatrix} x_1^{\hat{A}} + w \\ x_2^{\hat{A}} + \frac{l}{2} \\ -x_3^{\hat{A}} \end{bmatrix}$	$\begin{bmatrix} x_1^{\hat{A}} \\ x_2^{\hat{A}} + l \\ -x_3^{\hat{A}} \end{bmatrix}$

Table 6: $\mathrm{rUC}_{1/16}$: geometrical relations between equivalent points at the boundaries; l, w and t are respectively, the length width and and thickness of the rUC.

	$\hat{E}_1$	$\hat{E}_2$	$\hat{E}_3$	$\hat{E}_4$
$\mathbf{T}$	$\begin{bmatrix} -1 & 0 & 0 \\ 0 & -1 & 0 \\ 0 & 0 & -1 \end{bmatrix}$	$\begin{bmatrix} -1 & 0 & 0 \\ 0 & -1 & 0 \\ 0 & 0 & -1 \end{bmatrix}$	$\begin{bmatrix} -1 & 0 & 0 \\ 0 & -1 & 0 \\ 0 & 0 & 1 \end{bmatrix}$	$\begin{bmatrix} -1 & 0 & 0 \\ 0 & -1 & 0 \\ 0 & 0 & 1 \end{bmatrix}$
$\mathbf{x}^{O_{\hat{E}}}$	$\begin{bmatrix} w \\ 0 \\ 0 \end{bmatrix}$	$\begin{bmatrix} 0 \\ l \\ 0 \end{bmatrix}$	$\begin{bmatrix} -w \\ 0 \\ 0 \end{bmatrix}$	$\begin{bmatrix} 0 \\ -l \\ 0 \end{bmatrix}$
$\mathbf{x}^{\hat{A}}$	$\begin{bmatrix} \frac{w}{2} \\ -\frac{l}{2} \le y \le \frac{l}{2} \\ -\frac{t}{2} \le z \le \frac{t}{2} \end{bmatrix}$	$\begin{bmatrix} -\frac{w}{2} \le x \le \frac{w}{2} \\ \frac{l}{2} \\ -\frac{t}{2} \le z \le \frac{t}{2} \end{bmatrix}$	$\begin{bmatrix} -\frac{w}{2} \\ -\frac{l}{2} \le y \le \frac{l}{2} \\ -\frac{t}{2} \le z \le \frac{t}{2} \end{bmatrix}$	$\begin{bmatrix} -\frac{w}{2} \le x \le \frac{w}{2} \\ -\frac{l}{2} \\ -\frac{t}{2} \le z \le \frac{t}{2} \end{bmatrix}$
$\mathbf{x}^{A}$	$\begin{bmatrix} -x_1^{\hat{A}} + w \\ -x_2^{\hat{A}} \\ -x_3^{\hat{A}} \end{bmatrix}$	$\begin{bmatrix} -x_1^{\hat{A}} \\ -x_2^{\hat{A}} + l \\ -x_3^{\hat{A}} \end{bmatrix}$	$\begin{bmatrix} -x_1^{\hat{A}} - w \\ -x_2^{\hat{A}} \\ x_3^{\hat{A}} \end{bmatrix}$	$\begin{bmatrix} -x_1^{\hat{A}} \\ -x_2^{\hat{A}} - l \\ x_3^{\hat{A}} \end{bmatrix}$

Table 7: Admissible loadings cases and respective value of the load reversal factor for the rUCs analysed. For the OrUC, $\gamma_i = 1$, and all loadings are admissible.

	$\mathrm{rUC}_{1/8}$		$\mathrm{rUC}_{1/16}$	
	γ_i	Admissible loading	γ_i	Admissible loading
Case 1	$\begin{bmatrix} 1 & 1 & 1 & 1 & 1 & 1 \end{bmatrix}$	$\begin{bmatrix} \sigma_{11} & \sigma_{12} & 0 \\ \sigma_{21} & \sigma_{22} & 0 \\ 0 & 0 & \sigma_{33} \end{bmatrix}$	$\begin{bmatrix} 1 & 1 & 1 & 1 \end{bmatrix}$	$\begin{bmatrix} \sigma_{11} & \sigma_{12} & 0 \\ \sigma_{21} & \sigma_{22} & 0 \\ 0 & 0 & \sigma_{33} \end{bmatrix}$
Case 2	$\begin{bmatrix} 1 & -1 & -1 & 1 & -1 & -1 \end{bmatrix}$	$\begin{bmatrix} 0 & 0 & \sigma_{13} \\ 0 & 0 & \sigma_{23} \\ \sigma_{31} & \sigma_{32} & 0 \end{bmatrix}$	$\begin{bmatrix} 1 & 1 & -1 & -1 \end{bmatrix}$	$\begin{bmatrix} 0 & 0 & \sigma_{13} \\ 0 & 0 & \sigma_{23} \\ \sigma_{31} & \sigma_{32} & 0 \end{bmatrix}$

The FE analysis was performed using ABAQUS/Standard®. The loading given by Eq. 21 was applied, with $\varepsilon_{11} = 0.1$. Three different models were analysed: OrUC (defined in section 4.1), $\text{rUC}_{1/8}$ and $\text{rUC}_{1/16}$. Voxel meshing was used guaranteeing that the meshes of all models are exactly the same, i.e. physically equivalent regions are meshed similarly. This would be harder to assure if traditional meshing was used. Having identical meshes, the results obtained with the different models must be identical in order to confirm the boundary conditions are applied correctly. Figure 13 shows the results obtained with the different models are indeed identical. This can be further confirmed by comparing the value of ε_{11} obtained with the different domains along three paths defined on the surface of the load aligned tow. The oscillations/peaks are due to the unsmoothed nature of the voxel mesh used, it can be observed that, as expected, these peaks are exactly the same for all the models used. Figure 14 highlights the difference in computational time between models, showing the importance of using rUC for the efficient analysis of woven composites. This result is particularly relevant since, due to the nature of the structure being analyzed, the loading constraints of the smallest sub-domain are virtually not limiting for the analysis of this type of material.

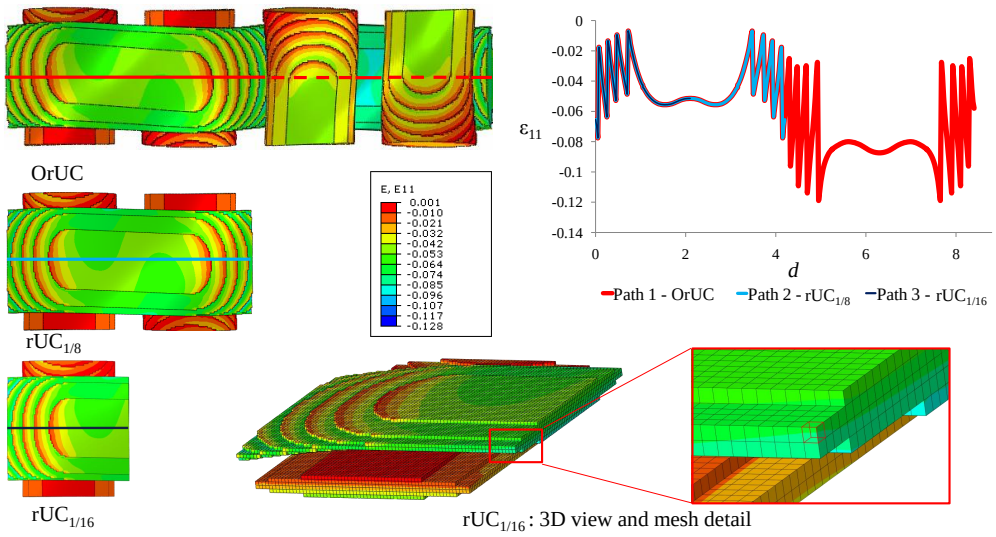

Figure 13: ε_{11} contour plot for the 2×2 Twill rUCs. The loading applied is given in Eq. 21. Paths 1-3 defined at surface of the longitudinal tow, similarly for different domains. The sharp variations verified are due to the unsmoothed nature of the voxel descretization used and are, as expected, exactly the same for the three models.

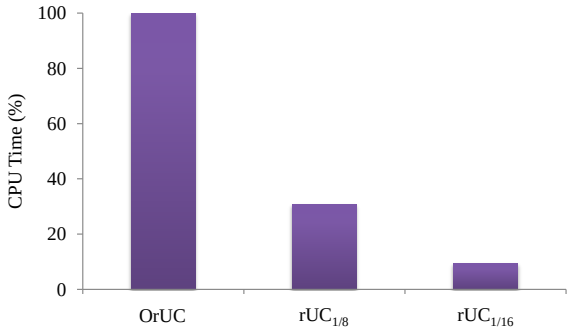

Figure 14: Comparison between the computational time spent on the three models analysed: OrUC, $rUC_{1/8}$ and $rUC_{1/16}$.

7. Conclusions

A theoretical framework leading to a sound derivation of PBCs for the analysis of domains smaller then the Unit Cells (UCs), named reduced Unit Cells (rUCs), by exploiting non-orthogonal translations and symmetries whithin the UC was developped. The investment in defining the problem formally resulted in a simple and readily usable formulation. The method is applied to 2D and 3D woven structures illustrating the potential of the rUC concept. Offset reduced Unit Cells are highlighted as a particular case with interesting features, allowing the analysis of domains smaller than the UC without any load restrictions. Additionally, OrUCs are particularly suitable for the analysis of 2D woven laminates, due to their independency on layer shifts and nesting.

The formulation proposed is used to develop an algorithm that: (i) automatically selects the smallest rUC for a given loading, (ii) determines and (iii) applies the appropriate periodic boundary conditions to the Finite Element Model of the rUC. Coupled with a voxel meshing procedure, it enables the automatic modelling and analysis of any 2D orthogonal weave.Albeit voxel meshing has advantages due to the ordered nature of the mesh obtained, the algorithm can be integrated with any other meshing procedure. Results show time savings of 90% can be achieved in the analysis stage, just by exploiting symmetries. In addition, time savings are also achieved in the modelling/meshing stages. The primitives of the algorithm are general and can be used for more complex structures.

The strategy proposed is a clear step towards the systematic and efficient numerical modelling of woven composites.

References

References

[1] S.V. Lomov, D.S. Ivanov, I. Verpoest, M. Zako, T. Kurashiki, H. Nakai, and S. Hirosawa. Meso-FE modelling of textile composites: Road map, data flow and algorithms. *Composites Science and Technology*, 67(9):1870–1891, July 2007.

[2] Z. Xia, Y. Zhang, and F. Ellyin. A unified periodical boundary conditions for representative volume elements of composites and applications. *International Journal of Solids and Structures*, 40(8):1907–1921, April 2003.

[3] Z. Xia, C. Zhou, Q. Yong, and X. Wang. On selection of repeated unit cell model and application of unified periodic boundary conditions in micro-mechanical analysis of composites. *International Journal of Solids and Structures*, 43(2):266 – 278, 2006.

[4] C.T. Sun and R.S. Vaidya. Prediction of composite properties from a representative volume element. *Composites Science and Technology*, 56(2):171–179, 1996.

[5] S. Li. Boundary conditions for unit cells from periodic microstructures and their implications. *Composites Science and Technology*, 68(9):1962 – 1974, 2008.

[6] S. Li. On the unit cell for micromechanical analysis of fibre-reinforced composites. *Proceedings: Mathematical, Physical and Engineering Sciences*, 455(1983):pp. 815–838, 1999.

[7] S. Li. General unit cells for micromechanical analyses of unidirectional composites. *Composites Part A: Applied Science and Manufacturing*, 32(6):815 – 826, 2001.

[8] S. Li and A. Wongsto. Unit cells for micromechanical analyses of particle-reinforced composites. *Mechanics of Materials*, 36(7):543 – 572, 2004.

[9] X. Tang and J.D. Whitcomb. General techniques for exploiting periodicity and symmetries in micromechanics analysis of textile composites. *Journal of Composite Materials*, 37(13): 1167–1189, 2003.

[10] S Li, C.V. Singh, and R. Talreja. A representative volume element based on translational symmetries for fe analysis of cracked laminates with two arrays of cracks. *International Journal of Solids and Structures*, 46(7-8):1793 – 1804, 2009.

[11] P. Suquet. Elements of homogenization theory for inelastic solid mechanics. In Sanchez-Palencia E. and Zaoui A., editors, *Homogenization Techniques for Composite Media*, Lecture Notes in Physics, pages 194–275. Springer-Verlag, Berlin., 1987.

[12] N.V. De Carvalho, S.T. Pinho, and P. Robinson. A mathematical framework for reducing the domain in the mechanical analysis of periodic structures. *arXiv:1012.3133v1*, pages 1–18, 2010.

[13] K.B. Breiling and D.O. Adams. Effects of layer nesting on compression-loaded 2D woven textile composites. *Journal of Composite Materials*, 30(15):1710–1728, October 1996.

[14] N.V. De Carvalho, S.T. Pinho, and P. Robinson. Compressive failure of 2D woven composites. In *17th International Conference on Composite Materials, 27 Jul - 31 Jul, Edinburgh, UK*, 2009.

[15] D.S. Ivanov, S.V. Lomov, S.G. Ivanov, and I. Verpoest. Stress distribution in outer and inner plies of textile laminates and novel boundary conditions for unit cell analysis. *Composites: Part A*, 41:571–580, 2010.

[16] E. Potter, S.T. Pinho, and P. Robinson. Unit cell mesh generation for 3D woven composites. *to be submitted*, 2008.

[17] *ABAQUS, Inc. ABAQUS version 6.9 Documentation. Dassault Systemes / SIMULIA (2010).*